MedChemComm

CONCISE ARTICLE

Received 00th January 20xx,

Accepted 00th January 20xx

DOI: 10.1039/x0xx00000x

www.rsc.org/

Spirooxadiazoline oxindoles with promising *in vitro* antitumor activities

C. J. A. Ribeiro, J. D. Amaral, C. M. P. Rodrigues, R. Moreira and M. M. M. Santos*

This paper reports the synthesis and biological evaluation of thirty one spirooxadiazoline oxindoles as potential anticancer agents. Nine compounds showed an antiproliferative activity below 10 μM, with four compounds more active than the positive control nutlin-3a in HCT 116 *p53*$^{(+/+)}$ cell line. Moreover, compound **1aa** was shown to induce p53 stabilization and transactivation, to induce apoptosis, and to inhibit the interaction between p53 and MDM2 in a live-cell bimolecular fluorescence complementation assay.

1. Introduction

Tumor suppressor p53 is a transcription factor widely regarded as the "guardian of the genome" that plays an important role in the regulation of several biological processes, including cell cycle arrest, apoptosis, DNA repair, senescence and metabolism.[1] Due to its unquestionable contribution to the preservation of genomic integrity, it is not surprising that tumor pathogenesis and development always seems to involve some sort of p53 impairment. Therefore, restoring p53 function in cancer cells represents a valuable anticancer approach.[2]

Pharmacological p53 reactivation strategies for cancer therapy can be clustered in two major approaches based on the cancer p53 status. When p53 is mutated (50% of all tumors), the most common strategy consists in refolding the protein into a wild-type conformation to restore its function. In tumors that retain wild-type p53 but have defects in p53 regulatory pathways, the main goal is to inhibit the function of its negative regulators, primarily MDM2 and MDM4.[3, 4]

Unlike common protein-protein interactions, in which the interface is large, and shallow,[5, 6] the MDM2-p53 interface consists of a deep hydrophobic cleft that can be targeted by small-molecule inhibitors.[7, 8] In fact, there are now seven MDM2 inhibitors (Fig. 1) in early phase clinical trials[9-12] for the treatment of human cancers, but the clinical proof concept has yet to be demonstrated. Generally, p53-MDM2 interaction inhibitors contain three lipophilic groups attached to a rigid heterocyclic scaffold to mimic the three most important p53 amino acids (Phe19, Trp23 and Leu26) that interact with MDM2. Furthermore, all the interactions are primarily hydrophobic, with potency increasing essentially by introduction of halide-substituted aromatic groups.[13] Heterocycles incorporating a spirooxindole framework are found in many natural products and medicinal agents with diverse biological activities.[14, 15] We recently reported several novel scaffolds, some containing a spirooxindole skeleton, with potential anticancer activity.[16-20] In particular, we have shown that spiroisoxazoline oxindoles are able to disrupt the interaction between p53-MDM2 in cell base assays.[17] Based on these positive results, we decided to investigate other potentially more active spirooxindoles containing different five-membered fused rings.

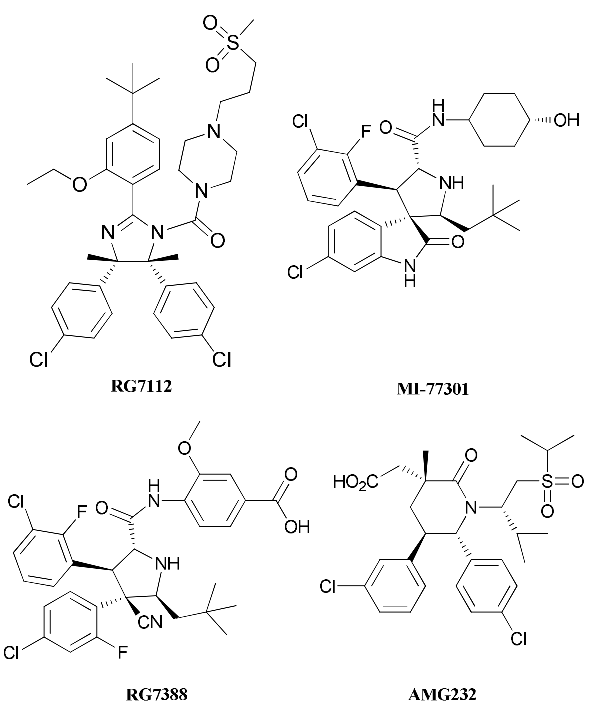

Fig. 1 Examples of p53-MDM2 interaction inhibitors currently in clinical trials.

Research Institute for Medicines (iMed.ULisboa), Faculty of Pharmacy, Universidade de Lisboa, Av. Prof. Gama Pinto, 1649-003 Lisboa, Portugal.
** E-mail: mariasantos@ff.ulisboa.pt*

Electronic Supplementary Information (ESI) available: synthetic procedure and characterization data of synthesized compounds; and *in vitro* biological activity procedures. See DOI: 10.1039/x0xx00000x

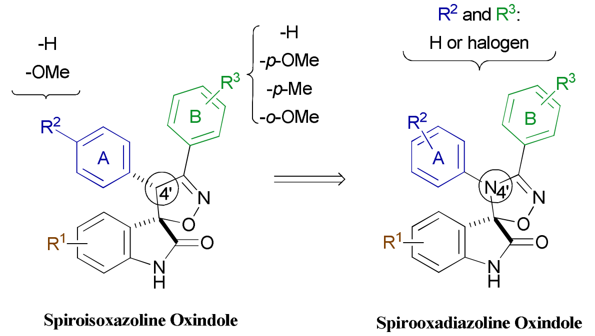

Scheme 1 Optimization Strategy.

Herein, we present the results obtained when the spiroisoxazoline carbon C-4', with tetrahedral molecular geometry, is substituted by a nitrogen atom (Scheme 1). This simple alteration abolishes a chiral center and reorients spatially the R^2 substituent. We also addressed two previous underexplored substitutions in the spiroisoxazoline oxindole scaffold: (*a*) probing the phenyl ring A that previously was limited to H and *p*-OMe, and (*b*) expand halogen substitutions outside the oxindole ring, since two vicinal halophenyl groups attached to a rigid heterocyclic core are a common feature among the published p53-MDM2 interaction disruptors.[21] Furthermore, we have developed derivatives with three aromatic side chains attached to the oxadiazoline moiety, in an attempt to mimic the three pivotal p53 amino acids that interact with MDM2.

2. Results and discussion

Chemistry

In our previous study the most active spiroisoxazoline derivative detained a halogen at position 6 of the oxindole,[17] which is in agreement with potent spiropyrrolidine oxindoles described in literature.[22] In addition, in other publications describing different spirooxindoles reported that a 5-halogen can sometimes be beneficial to increase anticancer activity.[23, 24] Therefore the first derivatizations were focused at these two positions. By probing R^2 and R^3, different spirooxadiazolines with 5-chlorooxindole (**1h-n, Table 1**) and 6-chlorooxindole (**1o-v**) moieties were initially synthesized. To validate the importance of having a halogen in the oxindole moiety, derivatives lacking this substituent were also tested (**1a-g**). In addition, and guided by these results, spirooxadiazolines detaining bromooxindole moiety (1**w-1ae**) were also synthesized and evaluated.

The spirooxadiazoline oxindoles (**1**, Scheme 2) were obtained in yields of 54–87%, by 1,3-dipolar cycloaddition between 3-imino-indolin-2-ones (**2**) and nitrile oxides generated *in situ* by dehydrohalogenation of hydroximoyl chlorides (**3**).[25, 26] The reaction proceeded in dichloromethane at room temperature. 3-Imino-indolin-2-ones (**2**) were synthesized by reacting indolin-2,3-diones (**4**) with different anilines (**5**) in ethanol at reflux, in the presence of acetic acid (61-93% yield).[27] Hydroximoyl chlorides (**3**) were synthesized starting from aromatic aldehydes (**6**). By reacting with hydroxylamine hydrochloride, in the presence of sodium carbonate, and in water at reflux, it formed first the corresponding aldoxime (**7**) *in situ*. Then, the reaction was followed by halogenation with *N*-chlorosuccinimide (NCS), using catalytic pyridine in chloroform at room temperature (71-91% yield).[28]

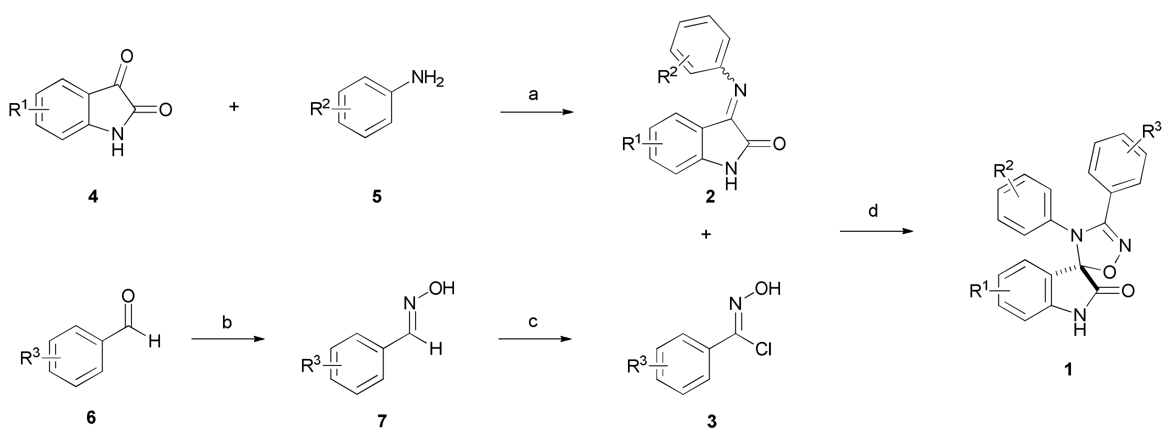

Scheme 2 Synthesis of spirooxadiazoline oxindole derivatives **1a–ae**. *Reagents and conditions*: (a) CH_3COOH, EtOH, reflux, 3-72h; (b) $NH_2OH{\cdot}HCl$, Na_2CO_3, H_2O, reflux, 2-5 h; (c) NCS, pyridine, CH_2Cl_2, r.t., 24h; (d) Et_3N, CH_2Cl_2, 5-12 h, r.t.

MedChemComm

CONCISE ARTICLE

Table 1. *In vitro* antiproliferative activities in HCT116 *p53*$^{(+/+)}$ cell line.

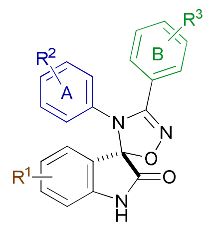

1

Compd	R^1	R^2	R^3	Yield (%)	HCT 116 *p53*$^{(+/+)}$ GI_{50}, μM[a]
1a	H	4-F	H	80	99.6±0.8
1b	H	3-Cl	H	82	70.1±3.2
1c	H	4-Cl	H	87	54.5±0.1
1d	H	3-Cl	3-Cl	85	32.6±0.4
1e	H	3-Cl	4-Cl	80	33.7±0.1
1f	H	4-Cl	3-Cl	84	38.4±2.4
1g	H	4-Cl	4-Cl	85	31.2±2.5
1h	5-Cl	H	H	76	39.1±2.0
1i	5-Cl	3-Cl	H	56	26.4±0.3
1j	5-Cl	3-Cl	3-Cl	54	4.6±0.2
1k	5-Cl	3-Cl	4-Cl	58	25.6±1.0
1l	5-Cl	4-Cl	H	69	27.1±2.5
1m	5-Cl	4-Cl	3-Cl	66	21.3±1.0
1n	5-Cl	4-Cl	4-Cl	64	17.6±0.5
1o	6-Cl	H	H	81	28.4±4.0
1p	6-Cl	H	4-Me	70	50.6±4.4
1q	6-Cl	H	4-Cl	82	26.5±0.1
1r	6-Cl	3-Cl	3-Cl	75	6.6±0.0
1s	6-Cl	3-Cl	4-Cl	78	20.2±1.0
1t	6-Cl	4-Cl	H	80	31.8±1.9
1u	6-Cl	4-Cl	3-Cl	80	28.7±2.1
1v	6-Cl	4-Cl	4-Cl	79	13.2±0.4
1w	5-Br	H	H	73	13.5±4.5
1x	5-Br	4-Cl	H	68	21.9±2.4
1y	5-Br	3-Cl	H	62	4.7±0.2
1z	5-Br	3-Cl	4-Cl	60	7.7±0.1
1aa	5-Br	3-Cl	3-Cl	61	2.0±0.0
1ab	5-Br	3-Br	3-Br	67	3.2±0.1
1ac	5-Br	3-Cl,4-F	3-Cl	55	6.6±0.2
1ad	5-Br	2-F,3-Cl	3-Cl	57	1.7±0.1
1ae	5-Br	3-Cl	2-F,3-Cl	61	3.2±0.3
Nutlin-3a					4.0±1.2

[a] GI_{50} determined by the MTS method after 72h. Each value is the mean (GI_{50} ± SD) of three independent experiments performed in duplicate.

Cellular activity and structure–activity relationships (SAR)

The tumor cell growth inhibitory potential of the spirooxadiazoline oxindoles and the contribution of the p53-pathway to their activities were thereafter ascertained using human colon adenocarcinoma HCT116 cell lines expressing wild-type p53 (HCT116 *p53*$^{(+/+)}$). The data obtained is presented on table 1.

All derivatives with 5-chloro and 6-chlorooxindole moieties were more potent than their unsubstituted oxindole equivalent (**1a-g**). Introduction of a second chloro at R^2 maintained or slightly increased the potency (**1i** and **1l** versus **1h**; **1t** versus **1o**). Moreover, the presence of an additional chloro, at R^3, led to an increase in potency when both halogens (ring A and B) were in *meta* or *para* positions, with the former representing an impressive 8.6-fold and 4.3-fold increase in potency when compared to the non-halogenated counterparts (**1j**, GI_{50}= 4.6 μM versus **1h**, GI_{50}= 39.1 μM and **1r**, GI_{50}= 6.6 μM versus **1o**, GI_{50}= 28.4 μM). Then we decided to test the effect of changing 5-chloro in the oxindole moiety to 5-bromo. As the best compound so far contained a 5-chlorooxindole (**1j**), the next set of compounds was focused in this position (**1w-aa**). Interestingly all compounds revealed to be more active than the 5-chlorooxindole equivalents, with three compounds reaching activities below 10 μM in HCT116 *p53*$^{(+/+)}$. As expected the most active compound in this series, **1aa** (GI_{50}= 2.0 μM), has two chlorine atoms in the *meta* positions of rings A and B, representing a 2-fold increase in comparison to **1j**. Changing both chlorine atoms for bromine slightly decreased the activity (**1ab**).

The next step was to introduce fluor atoms into phenyl rings A and B (**1aa-ab**), revealing that only 2-F,3-Cl in ring A promoted a slight increase in potency (**1ad**, GI_{50}= 1.7 μM), as expected by comparison to previously reported spiropyrrolidine oxindoles.[29]

Table 2. *In vitro* antiproliferative activities in HCT116 *p53*$^{(-/-)}$, HepG2 and SW620 cell lines

Compound	HCT116 *p53*$^{(-/-)}$ GI_{50}, µM[a]	HepG2 GI_{50}, µM[a]	SW620 GI_{50}, µM[a]	Compound	HCT116 *p53*$^{(-/-)}$ GI_{50}, µM[a]	HepG2 GI_{50}, µM[a]	SW620 GI_{50}, µM[a]
1i	41.6±2.0	-	-	**1x**	25.8±0.6	-	-
1j	6.8±0.7	3.3±0.3	3.9±0.4	**1y**	7.5±1.3	3.5±0.4	4.2±0.3
1k	29.0±0.6	-	-	**1z**	12.3±1.4	4.1±0.4	8.0±0.4
1l	27.0±2.7	-	-	**1aa**	2.9±0.2	2.1±0.0	2.1±0.3
1m	21.8±1.4	-	-	**1ab**	6.0±0.6	2.2±0.2	3.7±0.4
1n	18.0±0.8	-	-	**1ac**	7.2±0.5	4.0±0.4	6.7±0.2
1o	35.5±6.7	-	-	**1ad**	2.0±0.4	1.2±0.2	2.0±0.2
1q	30.6±1.3	-	-	**1ae**	4.4±0.8	2.5±0.06	3.5±0.04
1r	7.8±0.8	4.4±0.4	6.7±0.8	**Nutlin-3a**	47.8±1.9	-	-

[a] GI_{50} determined by the MTS method after 72h. Each value is the mean (GI_{50} ± SD) of three independent experiments performed in duplicate.

From the thirty one derivatives synthesized, four revealed to be more potent than the positive control nutlin-3a (**1aa-ab**, **1ad-ae**).

All compounds with GI_{50} lower than 30 µM were tested in HCT116 *p53*$^{(-/-)}$ cell line, in which p53 has been knocked out, and the derivatives with GI_{50} lower than 10 µM were additionally tested in two other cell lines: human hepatocellular carcinoma cell line (HepG2) that expresses wild-type p53 and a p53 mutant human colorectal adenocarcinoma cell line (SW620) (Table 2). Most compounds showed reduction of GI_{50} value in cell lines harbouring wild-type p53.

To investigate if spirooxadiazoline oxindole derivatives were capable of disrupting p53-MDM2 interaction, we applied a Venus-based bimolecular fluorescence complementation system methodology (BiFC) developed by our group.[30] We demonstrated that compound **1aa** can inhibit p53–MDM2 interaction in the same extent as nutlin-3a at concentrations of 10 and 20 µM (Fig. 2).

Direct protein-protein interaction between MDM2 and p53 regulates the basal levels and activity of p53 in cells through an autoregulatory feedback loop. Upon activation, p53 binds to *MDM2* gene promoter and transcriptionally induces MDM2 protein expression. In turn, MDM2 protein binds to p53 protein and inhibits it through multiple mechanisms: MDM2 blocks p53 transcription activity, exports p53 out of the nucleus, and promotes its proteosome-mediated degradation.[31]

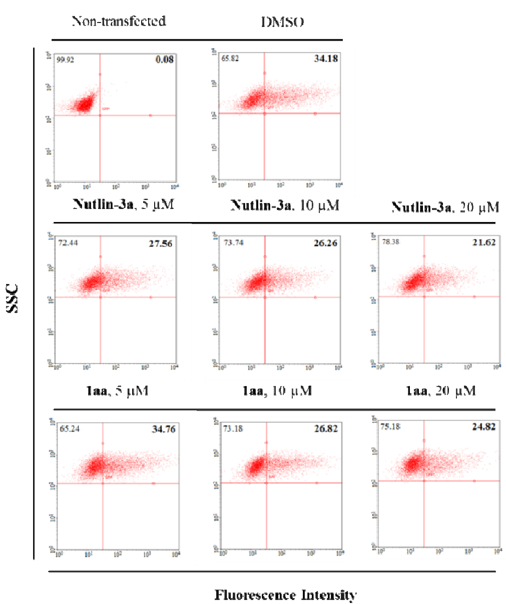

Figure 2. Compound **1aa** decreases p53-MDM2 interaction by BiFC. HCT116 *p53*$^{(-/-)}$ cells were co-transfected with V1-p53/MDM2-V2 BiFC combination plasmids for 24 h. Vehicle, nutlin-3a (5, 10, and 20 µM) and compound **1aa** (5, 10, and 20 µM) were included in the culture medium 4 h after transfection. Representative flow cytometry profiles of the disruption of V1-p53/MDM2-V2 complementation (n=3).

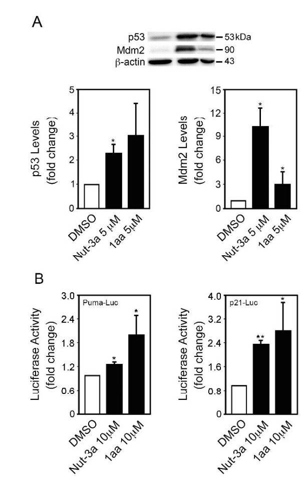

Figure 3. Compound **1aa** induces p53 stabilization and transcriptional activation in HCT116 *p53*$^{(+/+)}$ cells. *A*, Cells were incubated with vehicle, Nutlin-3a or compound **1aa** at 5 µM, for 24 h and total proteins processed for immunoblot analysis. Representative immunoblots of p53 and MDM2 protein levels. *B*, Cells were co-transfected with *PUMA* or *p21* promoter-driven luciferase reporter constructs containing p53 binding sites, in combination with pRL-SV40 renilla control vector, and treated 24 h after transfection with 10 µM Nutlin-3a and compound **1aa** for additional 24 h. The empty pBV-Luc vector was used as negative control. Reporter assays were performed 24 h post-treatment. Luciferase activity was normalized for transfection efficiency with control renilla expression. Blots were normalized

to endogenous β-actin. Data represent mean ± SEM of three independent experiments. *p < 0.05 and **p* < 0.001 from control with DMSO.

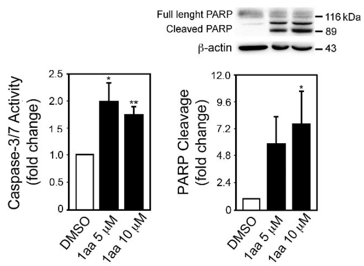

Figure 4. Compound **1aa** induces apoptosis. HCT116 *p53*$^{(+/+)}$ cells were incubated with vehicle, Nutlin-3a or compound **1aa** at 5 μM or 10 μM for 24 h. Total proteins were processed for immunoblot analysis and caspase-3/7 activity as described in ESI. Caspase-3 and -7 activities (*left*) and representative immunoblots of PARP cleavage (*right*). Blots were normalized to endogenous *β*-actin. Data represent mean ± SEM of three independent experiments. *p < 0.01 and ** p < 0.001 from control with DMSO.

Treatment of cells with compound **1aa** resulted in p53 stabilization and accumulation, and in a concomitant increase of MDM2 expression, as detected by Western blot analysis (Figure 3, A) ($p < 0.05$). The activation of p53 by compound **1aa** was further supported by transactivation of *PUMA*, a pro-apoptotic p53 transcriptional target gene, and *p21*, a p53-dependent mediator of cell cycle G_1 phase arrest (Figure 3, B). Caspase activation and cleavage of caspase-3 substrate PARP are also considered reliable markers of the apoptotic process.[32] Therefore, to confirm if our compounds induced cell death by apoptosis, we selected compound **1aa** to further study the molecular mechanism of action in HCT116 *p53*$^{(+/+)}$ tumor cell line. As depicted in Figure 4 compound **1aa** induced an activation of caspases-3 and -7 in a luminescent caspase-3/7 assay ($p < 0.05$). Moreover, this effect was accompanied by an increase of PARP cleavage as detected by Western blot (Figure 4) ($p < 0.05$). Finally, incubation with compound **1aa** did not induce p53 Ser^{15} phosphorylation (see ESI), suggesting a nongenotoxic mechanism of p53 activation, as reported for Nutlins.[33]

Stability

Chemical stability in pH 7.4 phosphate buffer and metabolic stability in human plasma and rat liver microsomes at 37 ºC were evaluated for compound **1ad**. The compound was stable in phosphate buffer for the duration of the assays (3 days), and showed good stability in plasma with only 38% degradation after 72 h of incubation. Compound **1ad** was moderately metabolized when incubated in rat microsomes with NADPH regenerating system, with half-lives of 33.5±2.6 min, indicating great susceptibility towards co-factor dependent microsomal enzymes.

Conclusions

Thirty one compounds were synthesized with different substituents attached to the spirooxadiazoline oxindole scaffold. Screening the compounds in HCT116 *p53*$^{(+/+)}$ cell line revealed that nine derivatives displayed potency below 10 μM, and four derivatives were more potent than the positive control nutlin-3a (GI_{50} bellow 4.0 μM). The best compounds possessed halogen in positions 5 or 6 of the oxindole and *meta*-halogens in rings A and B. The most active compound (**1ad**) showed a GI_{50} of 1.7 μM in HCT116 *p53*$^{(+/+)}$ cell line, representing an 15.4-fold increase in potency when compared to the most active spiroisoxazoline oxindole obtained previously (HCT116 *p53*$^{(+/+)}$ GI_{50}= 26.6 μM).[17] Together, the results obtained in HCT116 tumor cells indicated that spirooxadiazoline oxindoles reduce the p53 inhibition by MDM2, subsequently increasing the expression levels of p53 target genes.

Acknowledgements

This study was supported by FCT (Fundação para a Ciência e a Tecnologia, Portugal) by research projects PTDC/QUI QUI/111664/2009, PTDC/SAU-FAR/110848/2009, PTDC/ SAU-ORG/119842/2010 and UID/DTP/04138/2013, and by fellowships: SFRH/BD/69258/2010 (C.J.A.R.) and SFRH/BPD/100961/2014 (J.D.A.). M. M. M. Santos would like to acknowledge FCT, "Programa Operacional Potencial Humano" and the European Social Fund for the IF Program (IF/00732/2013).

References

1. A. J. Levine and M. Oren, *Nat. Rev. Cancer*, 2009, **9**, 749-758.
2. K. K. Hoe, C. S. Verma and D. P. Lane, *Nat. Rev. Drug Discov.*, 2014, **13**, 217-236.
3. B. Hong, A. P. J. van den Heuvel, V. V. Prabhu, S. Zhang and W. S. El-Deiry, *Curr. Drug. Targets*, 2014, **15**, 80-89.
4. J. Zawacka-Pankau and G. Selivanova, *J. Intern. Med.*, 2015, **277**, 248-259.
5. M. R. Arkin, Y. Tang and J. A. Wells, *Chem. Biol.*, 2014, **21**, 1102-1114.
6. M. Pelay-Gimeno, A. Glas, O. Koch and T. N. Grossmann, *Angew. Chem. Int. Ed.*, 2015, **54**, 8896-8927.
7. Y. Zhao, A. Aguilar, D. Bernard and S. Wang, *J. Med. Chem.*, 2015, **58**, 1038-1052.
8. P.-C. Lv, J. Sun and H.-L. Zhu, *Curr. Med. Chem.*, 2015, **22**, 618-626.
9. B. Vu, P. Wovkulich, G. Pizzolato, A. Lovey, Q. J. Ding, N. Jiang, J. J. Liu, C. L. Zhao, K. Glenn, Y. Wen, C. Tovar, K. Packman, L. Vassilev and B. Graves, *ACS Med. Chem. Lett.*, 2013, **4**, 466-469.
10. S. Wang, W. Sun, Y. Zhao, D. McEachern, I. Meaux, C. Barriere, J. A. Stuckey, J. L. Meagher, L. Bai, L. Liu, C. G. Hoffman-Luca, J. Lu, S. Shangary, S. Yu, D. Bernard, A. Aguilar, O. Dos-Santos, L. Besret, S. Guerif, P. Pannier, D. Gorge-Bernat and L. Debussche, *Cancer Res.*, 2014, **74**, 5855-5865.
11. Q. Ding, Z. Zhang, J.-J. Liu, N. Jiang, J. Zhang, T. M. Ross, X.-J. Chu, D. Bartkovitz, F. Podlaski, C. Janson, C. Tovar, Z.

M. Filipovic, B. Higgins, K. Glenn, K. Packman, L. T. Vassilev and B. Graves, *J. Med. Chem.*, 2013, **56**, 5979-5983.

12. D. Sun, Z. Li, Y. Rew, M. Gribble, M. D. Bartberger, H. P. Beck, J. Canon, A. Chen, X. Chen, D. Chow, J. Deignan, J. Duquette, J. Eksterowicz, B. Fisher, B. M. Fox, J. Fu, A. Z. Gonzalez, F. G.-L. De Turiso, J. B. Houze, X. Huang, M. Jiang, L. Jin, F. Kayser, J. Liu, M.-C. Lo, A. M. Long, B. Lucas, L. R. McGee, J. McIntosh, J. Mihalic, J. D. Oliner, T. Osgood, M. L. Peterson, P. Roveto, A. Y. Saiki, P. Shaffer, M. Toteva, Y. Wang, Y. C. Wang, S. Wortman, P. Yakowec, X. Yan, Q. Ye, D. Yu, M. Yu, X. Zhao, J. Zhou, J. Zhu, S. H. Olson and J. C. Medina, *J. Med. Chem.*, 2014, **57**, 1454-1472.
13. G. M. Popowicz, A. Doemling and T. A. Holak, *Angew. Chem. Int. Ed.*, 2011, **50**, 2680-2688.
14. M. M. M. Santos, *Tetrahedron*, 2014, **70**, 9735-9757.
15. B. Yu, D. Q. Yu and H. M. Liu, *Eur. J. Med. Chem.* 2015, **96**, 673-698.
16. C. J. A. Ribeiro, S. P. Kumar, R. Moreira and M. M. M. Santos, *Tetrahedron Lett.*, 2012, **53**, 281-284.
17. C. J. A. Ribeiro, J. D. Amaral, C. M. P. Rodrigues, R. Moreira and M. M. M. Santos, *Bioorg. Med. Chem.*, 2014, **22**, 577-584.
18. A. Monteiro, L. M. Goncalves and M. M. M. Santos, *Eur. J. Med. Chem.*, 2014, **79**, 266-272.
19. J. Soares, N. A. L. Pereira, A. Monteiro, M. Leao, C. Bessa, D. dos Santos, L. Rairnundo, G. Queiroz, A. Bisio, A. Inga, C. Pereira, M. M. M. Santos and L. Saraiva, *Eur. J. Pharm. Sci.* 2015, **66**, 138-147.
20. J. Soares, L. Raimundo, N. A. Pereira, D. J. dos Santos, M. Perez, G. Queiroz, M. Leao, M. M. Santos and L. Saraiva, *Pharmacol. Res.*, 2015, **95-96**, 42-52.
21. K. Khoury, G. M. Popowicz, T. A. Holak and A. Doemling, *Med. Chem. Comm*, 2011, **2**, 246-260.
22. Y. Zhao, S. Yu, W. Sun, L. Liu, J. Lu, D. McEachern, S. Shargary, D. Bernard, X. Li, T. Zhao, P. Zou, D. Sun and S. Wang, *J. Med. Chem.*, 2013, **56**, 5553-5561.
23. A. Kumar, G. Gupta, A. K. Bishnoi, R. Saxena, K. S. Saini, R. Konwar, S. Kumar and A. Dwivedi, *Bioorg. Med. Chem.*, 2015, **23**, 839-848.
24. A. Bertamino, M. Soprano, S. Musella, M. R. Rusciano, M. Sala, E. Vernieri, V. Di Sarno, A. Limatola, A. Carotenuto, S. Cosconati, P. Grieco, E. Novellino, M. Illario, P. Campiglia and I. Gomez-Monterrey, *J. Med. Chem.*, 2013, **56**, 5407-5421.
25. A. Franke, *Justus Liebigs Ann. Chem.*, 1978, 717-725.
26. J. Azizian, K. Jadidi, M. Mehrdad and Y. Sarrafi, *Synthetic Commun*, 2000, **30**, 2309-2315.
27. A. H. Abadi, S. M. Abou-Seri, D. E. Abdel-Rahman, C. Klein, O. Lozach and L. Meijer, *Eur. J. Med. Chem.*, 2006, **41**, 296-305.
28. A. V. Dubrovskiy and R. C. Larock, *Org Lett*, 2010, **12**, 1180-1183.
29. Z. Zhang, X.-J. Chu, J.-J. Liu, Q. Ding, J. Zhang, D. Bartkovitz, N. Jiang, P. Karnachi, S.-S. So, C. Tovar, Z. M. Filipovic, B. Higgins, K. Glenn, K. Packman, L. Vassilev and B. Graves, *ACS Med. Chem. Lett.*, 2014, **5**, 124-127.
30. J. D. Amaral, F. Herrera, P. M. Rodrigues, P. A. Dionisio, T. F. Outeiro and C. M. Pereira Rodrigues, *Biochem. Pharmacol.*, 2013, **85**, 745-752.
31. M. Wade, Y.-C. Li and G. M. Wahl, *Nat. Rev. Cancer*, 2013, **13**, 83-96.
32. M. Germain, E. B. Affar, D. D'Amours, V. M. Dixit, G. S. Salvesen and G. G. Poirier, *J. Biol. Chem.*, 1999, **274**, 28379-28384.
33. L. T. Vassilev, B. T. Vu, B. Graves, D. Carvajal, F. Podlaski, Z. Filipovic, N. Kong, U. Kammlott, C. Lukacs, C. Klein, N. Fotouhi and E. A. Liu, *Science*, 2004, **303**, 844-848.

Spirooxadiazoline oxindoles were synthesized and evaluated for antitumor activity.